Progress report by Ramos and Dobry at RPI
Material to be included in Ricardo Ramos
(1999) Ph. D. Thesis at RPI

Update Progress on NCEER Highway Project

Centrifuge Modeling of Liquefaction Effects

Project 106

Task 106-E-4.11

July 21, 1998

Introduction:

Abdoun (1997) and Dobry and Abdoun (1998) studied the effect of lateral spreading on end bearing single piles without any restraint at the top of the pile. The setup of their centrifuge model test is shown in Fig. 1. The bending moments in the pile due to the liquefied soil pressure were measured at different points along the pile. From the measured maximum moments, Dobry and Abdoun found that the pressure exerted by the soil per unit area of the pile has an approximately triangular shape with depth, with a maximum pressure of 17.7 kN/m^2 occurring at the top of the pile (Fig. 2). This task continues Abdoun's (1997) work, by considering the effect of a restraining element above the ground surface simulating the stiffness of the bridge deck in the direction of the lateral spread (typically the longitudinal stiffness of the bridge).

Return to Table of Contents

Effect of the bridge deck stiffness on pile foundation with lateral spreading.

Experimental setup:

A series of three centrifuge tests (Test #2, Test #3 and Test #4) have already been conducted to study the effect of the bridge stiffness on the pile foundation subjected to lateral spreading. The basic setup is presented in Fig. 3. The bridge stiffness is modeled as a horizontal spring connected to the top of the pile (element ABC). The RPI flexible laminar box container is used. To facilitate comparison of the results, the setup of this experiment is essentially identical to that in Fig. 1 done by Abdoun, except for restraining element ABC. The model consists of an individual end-bearing pile going through a uniform liquefiable sand layer. The prototype single pile being simulated is 60 cm in diameter, 8 m in length, has a bending stiffness, EI = 8000 kN-m^2, and is embedded in the two-layer soil system. The displacement at the top of the pile is restrained by spring ABC. The bending moments are measured at six positions along the pile using strain gauges SG1 to SG6. The displacement at the restraint AB is measured using LVDT6. The soil deformations in the free field are measured by connecting LVDTs to the laminar box rings (LVDT1 to LVDT5). The prototype soil profile consists of 6 m layer of Nevada sand saturated with water, having a relative density of about 40%, and placed on top of a 2 m slightly cemented sand layer. The soil is instrumented with piezometers PPT1 and PPT2. Two accelerometers are connected to the rings (A4 and A5), while two accelerometers measure accelerations in the liquefied soil (A2 and A3). The whole

Return to Table of Contents

model is slightly inclined to the horizontal to induce lateral spreading. A prototype input acceleration of 0.3g and a frequency of 2 Hz was applied to the base.

A rectangular steel bar AB was used as the horizontal spring at the top of the pile. This steel bar AB is fixed to the laminar box at point A, and acts as a cantilever beam. The bending stiffness of the steel bar is used as the horizontal stiffness of the spring at the top of the pile. The end of the steel bar is then connected by a horizontal rigid link to the pile. Both connections, at the pile (point C) and at the steel bar (point B), were done as pin connection so that the pile is free to rotate.

Results

First the free field displacements are compared in order to verify the repeatability of all test considered. Figure 4 presents the free field displacements at end of shaking measured in Tests #2 through #4, as well as in the test done by Abdoun (1997) without restraint at the top. It can be observed that the results from all tests are very consistent.

The free field soil displacements vs. time, and the displacement at the restraint vs. time, measured in Test #2, are presented in Fig. 5. The maximum measured displacement at the restraint was 21.5 cm in prototype units and occurred at about 6 seconds. This is similar to the behavior observed by Abdoun (1997) in his test without a restraint, where the displacement of the top of the pile also increased and then decreased during shaking

Figure 6 presents the bending moments vs. time measured in Test #2 by strain gauges SG1 through SG6. The maximum bending moment occurs at the interface between the cemented layer and the sand, at depth of about 6m. As expected, this maximum bending moment and the maximum displacement at the restraint at top of the

Return to Table of Contents

pile occur simultaneously. Again, this is qualitatively similar to the behavior observed by Abdoun (1997) in his test. However, the moments in Fig. 6 are smaller than those measured in Abdoun's test. While Abdoun measured a maximum moment of 113 kN-m at 6m depth, the corresponding moment for Test #2 is only 85 or 86 kN-m.

The structural model used to analyze the measured moment distribution in Test #2 represents the pile as a vertical cantilever beam fixed at the interface between the cemented layer and the sand, loaded with the inverted triangular load of Fig. 2, and with a concentrated resisting lateral force, F, caused by the resistance of the spring at the top of the beam. The magnitude of the force F is known at the time of the maximum moment, because both the stiffness of the spring and the displacement of the spring are known. This horizontal force F acts 0.85m above the ground surface. The horizontal spring stiffness in Test #2 is 0.208 kN/cm, and the maximum displacement measured was 21.5 cm. Therefore, the maximum moment at the interface, that is at $z = 6$ m depth, and for a pile diameter $d = 0.6$ m, is predicted to be:

$$\begin{aligned} M_{max} &= (0.6\text{m})(0.5)(6.0\text{m})(17.7\text{kN}/\text{m}^2)(2/3)6 - (0.208\text{kN}/\text{cm})(21.5\text{cm})(6.85\text{m}) \quad \text{Eq. 1} \\ &= 127.44 - 30.63 = 96.81\ \text{kN}-\text{m} \end{aligned}$$

For other depths, z, the maximum moment, M_{max}, is predicted by:

for $-0.85 < z < 0\text{m}$

$$M_{max}(z) = -0.208(21.5)(z + 0.85) \qquad \text{Eq. 2}$$

for $0 \le z \le 6.85\text{m}$

$$M_{max}(z) = \frac{0.6(17.7)(6-z)z^2}{12} + 0.6\left(17.7 - \frac{(17.7)(6-z)}{6}\right)\frac{z^2}{3} - 0.208(21.5)(z+0.85) \qquad \text{Eq. 3}$$

A comparison between the analytical expression and the results obtained from Test #2 is shown in Fig. 8. It can be observed that the analytical expression is in good

Return to Table of Contents

agreement with the values obtained from the test. This verifies the hypothesis of Dobry and Abdoun (1998) that the pressure of the liquefied soil on the pile follows a triangular distribution with a maximum value of 17.7 kN/m^2 at the top.

It is interesting that without the presence of the force at the restraint, the predicted moment at z = 6m is 118.96 kN-m, very similar to M_{max} = 113 kN-m measured by Abdoun without the restraint, with the reduction between this value and 96.81 kN-m fully explained by the model.

Future work:

- Change the diameter of the pile to verify that the maximum pressure of the liquefied soil is still 17.7 kN/m^2, independent of pile diameter.
- Increase the spring stiffness.
- Do experiments with a three-layer soil system (cemented layer – saturated loose sand – cemented layer) with a restraint at the top of the pile.

References:

Abdoun, T. (1997). "Modeling of Seismically Induced Lateral Spreading of Multi-Layer Soil Deposit and Its Effect on Pile Foundations," Ph.D. Thesis, Dept. of Civil Engineering, Rensselaer Polytechnic Institute, Troy, NY

Dobry, R. and Abdoun, T. (1998). "Post-Triggering Response of Liquefied Sand in the Fee Field and Near Foundations," Proceedings, Third ASCE Specialty Conference on Geotechnical Engineering and Soil Dynamics, Seattle, WA, August 3-8, 1998.

Return to Table of Contents

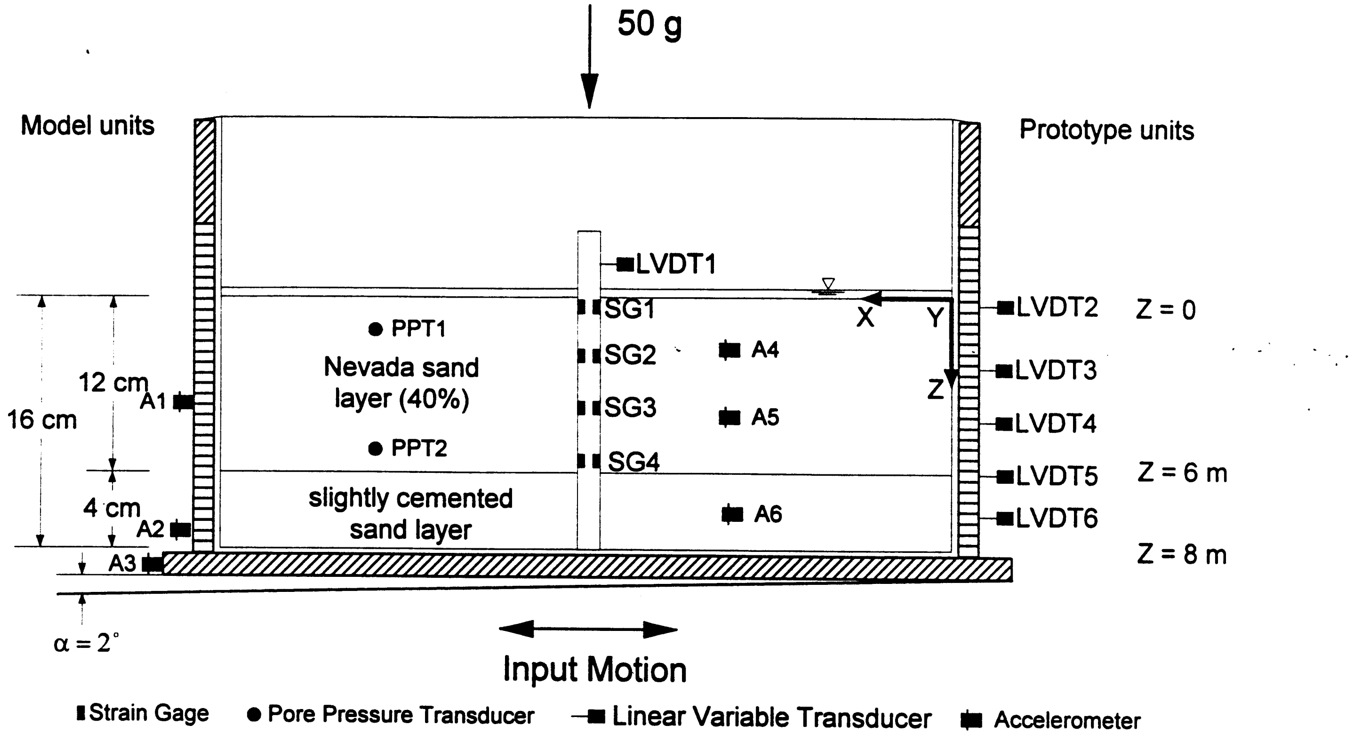

Figure 1.

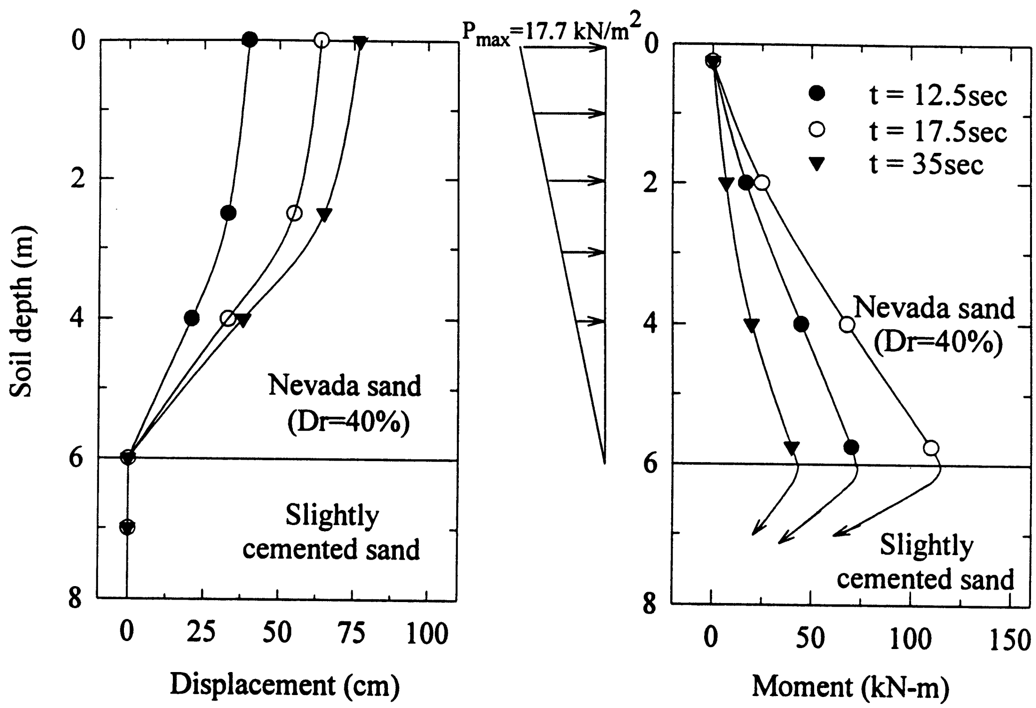

Figure 2.

Return to Table of Contents

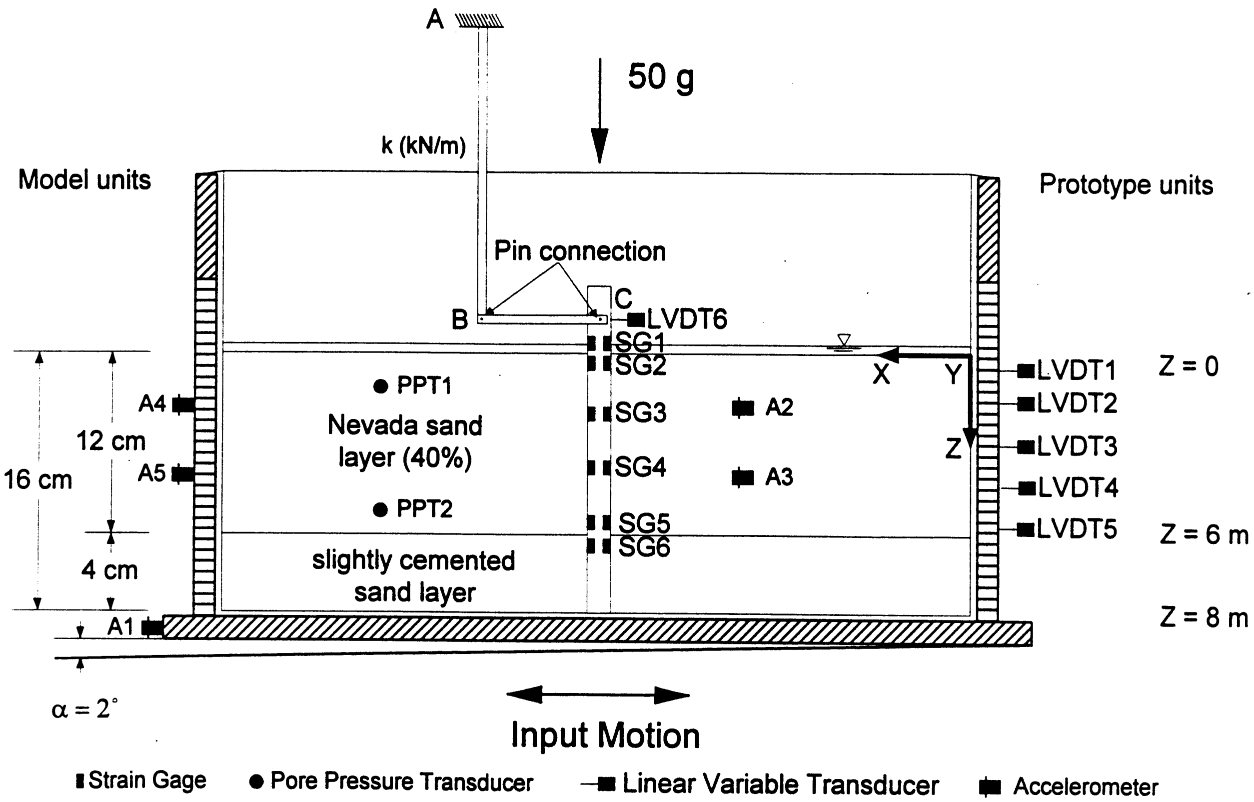

Figure 3

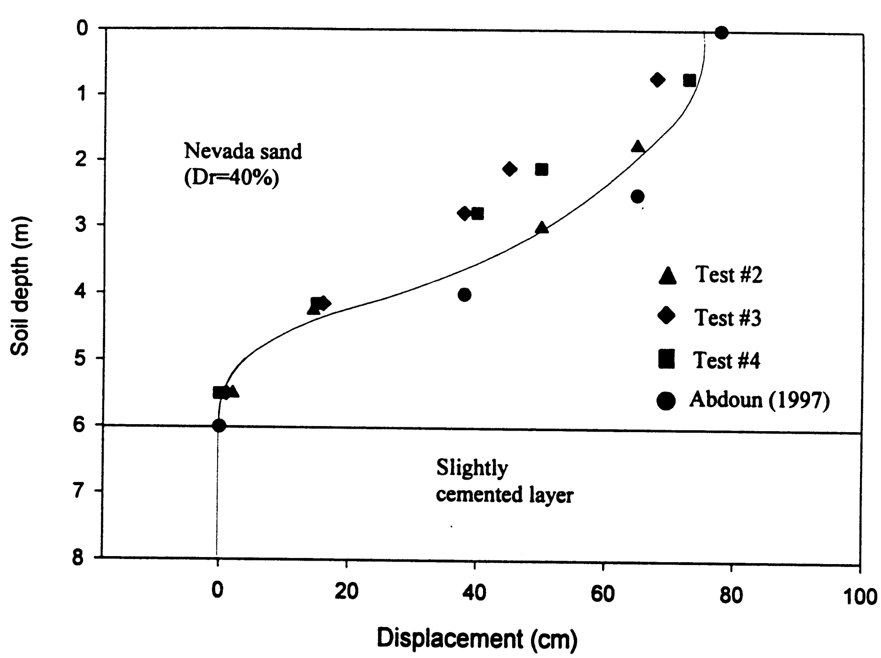

Figure 4.

Return to Table of Contents

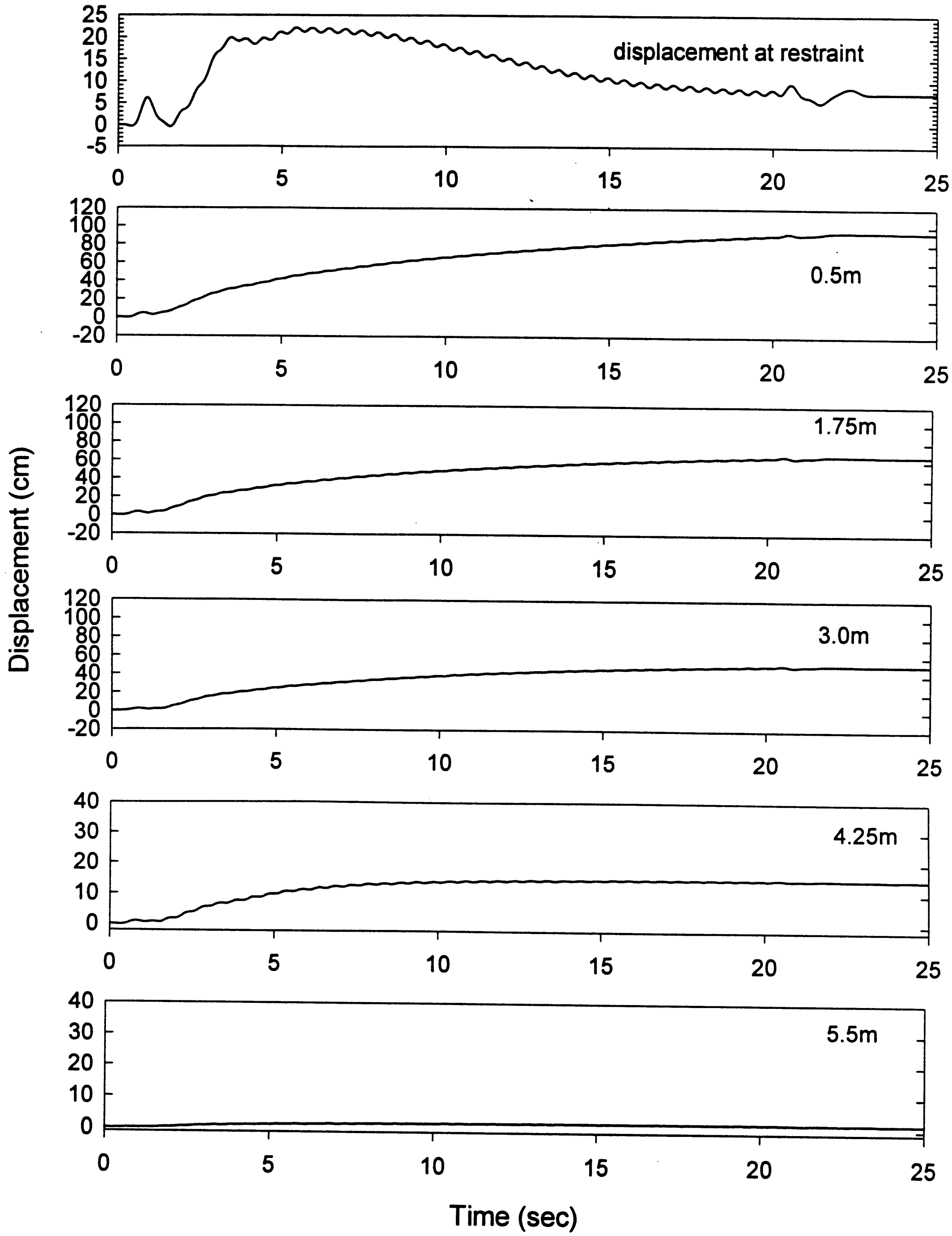

Figure 5.

Return to Table of Contents

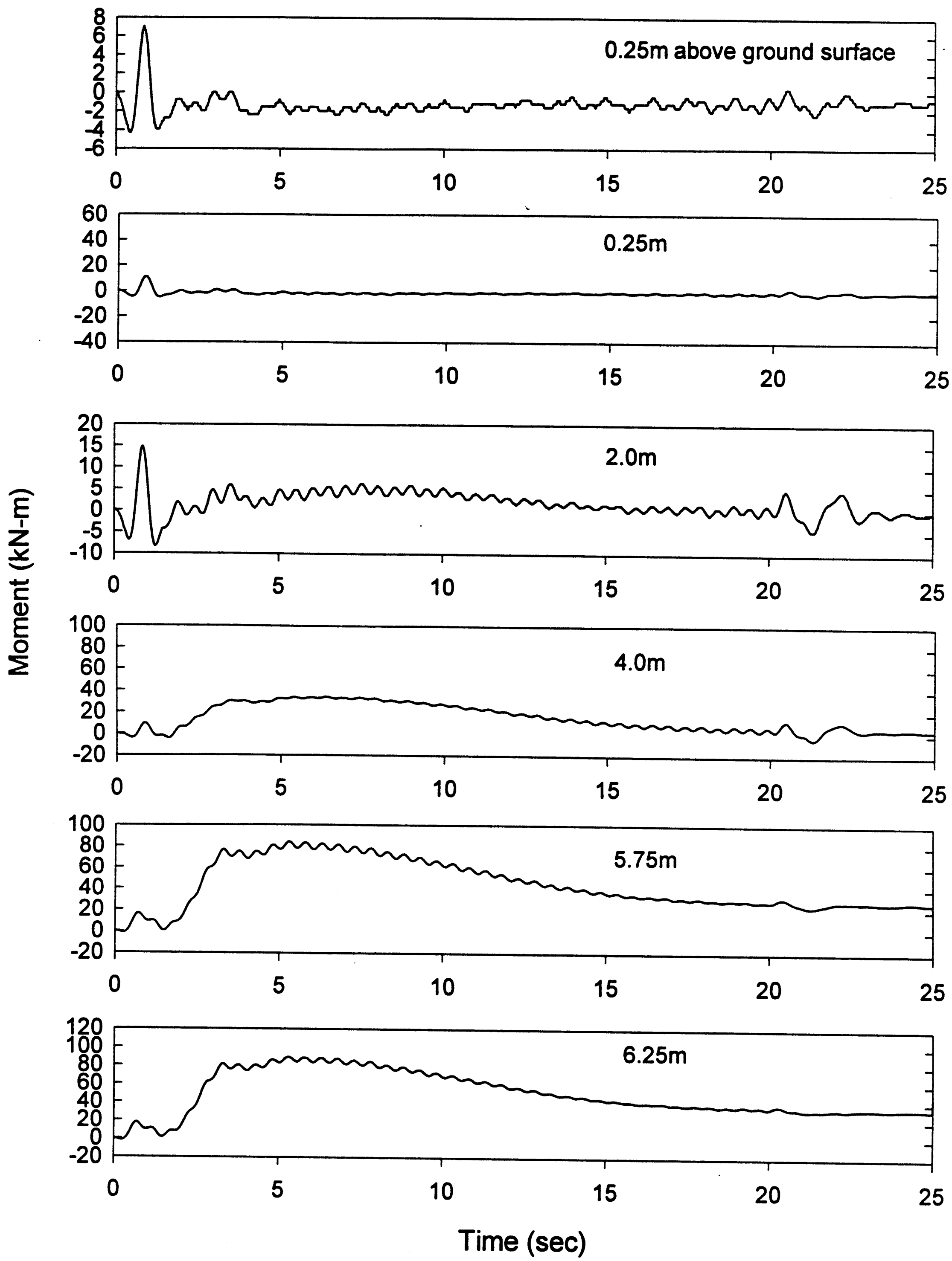

Figure 6.

Return to Table of Contents

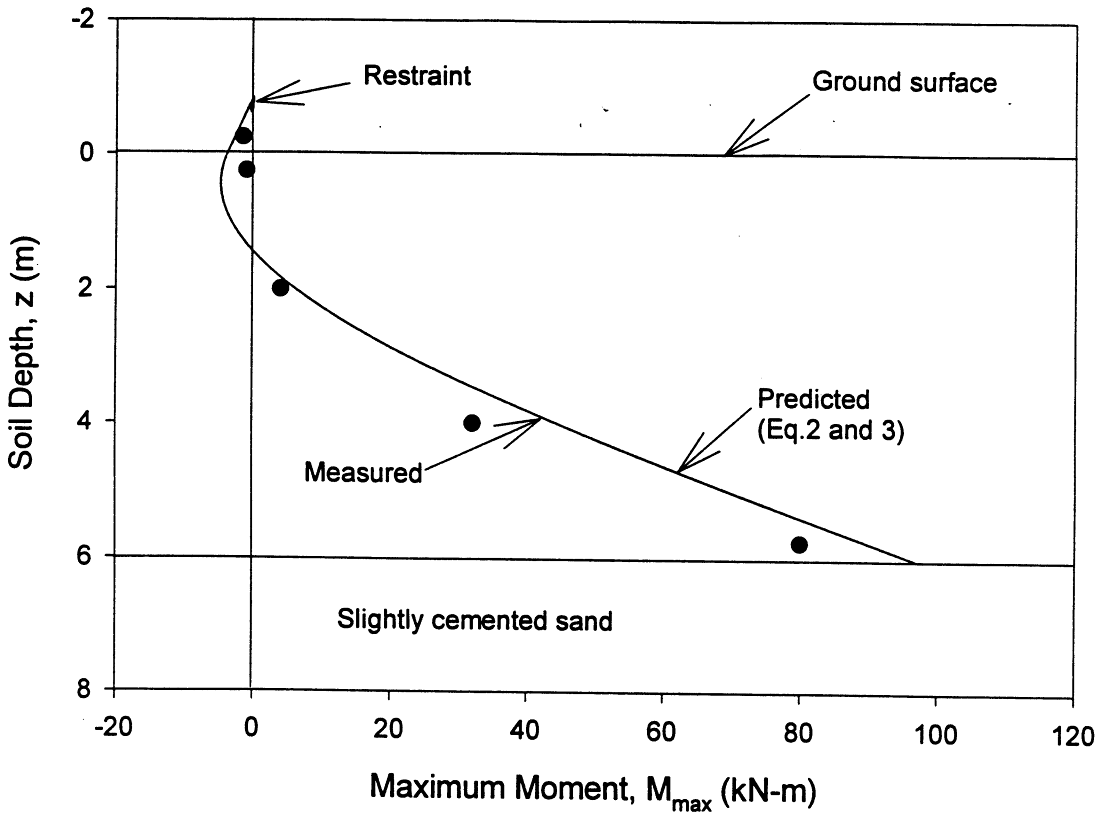

Figure 7.

Return to Table of Contents